Available online at www.sciencedirect.com
SCIENCE DIRECT®
Journal of Power Sources 146 (2005) 349–354
JOURNAL OF POWER SOURCES
www.elsevier.com/locate/jpowsour

A comparison between intercalation of Li and Mg ions into the model Chevrel phase compound ($M_xMo_6S_8$): Impedance spectroscopic studies

M.D. Levi *, D. Aurbach

Department of Chemistry, Bar-Ilan University, 52900 Ramat-Gan, Israel

Available online 27 April 2005

Abstract

Comparison between Li and Mg ions insertion into the Chevrel phase $M_xMo_6S_8$ (M = Li, Mg) shows interesting features related to the different interactions of the monovalent and the divalent ions with the Mo clusters and the anionic framework. It is clear that Mg ions insertion is much more complicated than Li ions insertion. An attempt was made to explain the peculiar behavior of the impedance spectra related to Mg ions insertion into the Mo_6S_8 electrode by a recent model for two non-equivalent lattice sites with two different energy barriers, which predicts the so-called "Gerischer-type impedance" at high frequencies and at the low-frequencies the appearance of additional semicircle, the latter being especially pronounced at the beginning of intercalation. We measure a charge-trapping of the Mg ions in the Chevrel phase at the initial stage of intercalation and at the final stage of deintercalation. An increase in the intercalation level (accompanied by a decrease in potential) correlates with a decrease in the trapping resistance, R_{trap}. We explain these features of the impedance response of the Mg ions insertion by the peculiar nature of the sites for small ions accommodation in the Chevrel phase structure. The divalent nature of the Mg-ions leads to their slower diffusion compared to the single charge Li ions. In general, the diffusion barrier of the trapped ions decreases with the increase in concentration due to the high electrostatic repulsion among the divalent cations.

Keywords: Electrochemical impedance; Mg-ion intercalation; Ion trapping; Gerischer impedance

1. Introduction

We have recently presented an extensive comparative study of Li and Mg ions insertions into Mo_6S_8 Chevrel phase compounds using a combination of three major electroanalytic techniques [1–3]. Fig. 1 demonstrates a comparison between the voltammetric behavior of Li and Mg insertion into Mo_6S_8 Chevrel phase (a and b, respectively). It is seen from this figure that whereas intercalation of Li ions occurs reversibly via three first-order phase transitions (note three reversivle redox-peaks a/a′, b/b′, and c/c′ in Fig. 1a), Mg ions intercalation was found to occur via two first-order phase transitions (2 redox-peaks a/a′ and b/b′ in Fig. 1b). The initial magnetization (final demagnetization) revealed a very slow kinetics with considerable charge-trapping at ambient (25 °C) temperature. The reversibility of Mg ions insertion, however, drastically increases at higher intercalation levels, so that the second Mg-ions transfer (i.e. the transfer from $Mg_1Mo_6S_8$ to $Mg_2Mo_6S_8$) proceeds under quasi-equilibrium conditions. We suspect that the above slow initial kinetics of Mg-ion insertion is somehow connected to the trapping of the divalent cations by the clustered matrix of the Chevrel phase host. The polarizability of the sulfide anionic framework may be too small to allow low enough diffusion barriers during the first stage of Mg ions intercalation. Neutron diffraction analysis of lithiated Mo_6S_8, revealed [4] that there are two types of sites for small ions accommodation in this host, namely, a six-sites inner and six-sites outer rings. Each ring of six sites can host one Mg ion (totally 2 Mg ions per a Mo_6S_8 unit). These two sets may be responsible for the fact that we see two types of diffusion processes (initial—slow and further fast).

We also performed an extensive EIS study of Mg ions insertion into Mo_6S_8, showing that trapping of ions was always accompanied by large low-frequency semicircles (LFSs) [3].

* Corresponding author. Tel.: +972 353 183 0910; fax: +972 353 51250.
E-mail address: levimi@mail.biu.ac.il (M.D. Levi).

0378-7753/$ – see front matter © 2005 Elsevier B.V. All rights reserved.
doi:10.1016/j.jpowsour.2005.03.014

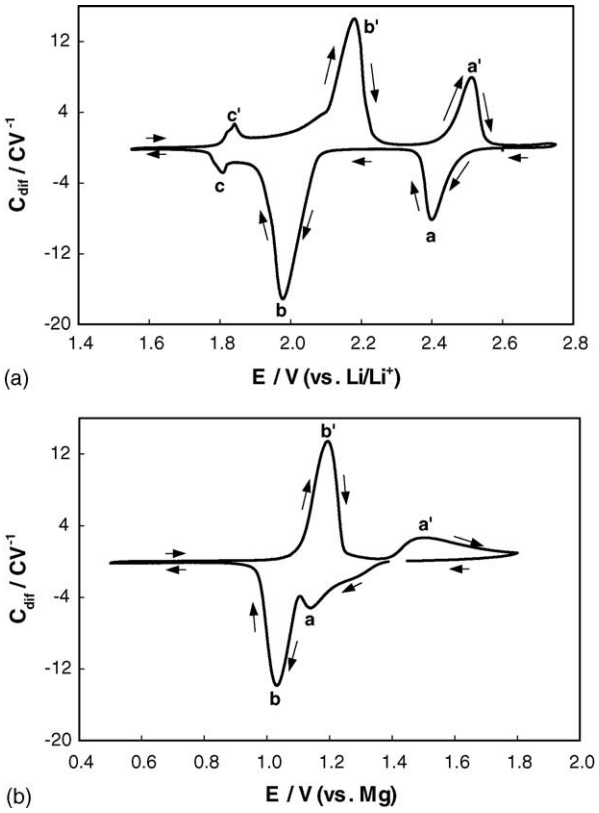

Fig. 1. SSCV curves measured at 25 μV s^{-1} for the insertion of Li (a) and Mg ions (b) from 1 M $LiClO_4$/PC and 0.25 M $Mg(AlCl_2EtBu)_2$ (DCC)/THF solutions, respectively. The active mass of the Mo_6S_8 Chevrel phase in both cases was close to 10 mg. Phase transitions occur along the redox-peaks a/a′, b/b′, c/c′ for Li ions insertion, and along the peaks a/a′ and b/b′ for Mg ions insertion.

The increase in the intercalation level results in a drastic decrease in the diameters of these LFSs. Simultaneously, we found evidence that at higher frequencies, the LFS semicircles transformed into a Gerischer-type impedance, although the way in which these two elements of impedance structure stuck, remained unclear (the "length" of the Gerischer-type impedance with respect to frequency was clearly potential-dependent [3]). The study described herein is aimed at progressing our understanding of the impedance behavior of intercalation electrodes.

In the present paper, we show that a modification of the two energy state model describing the coupling of solid state ion diffusion and ion trapping processes presented in full detail by Bisquert and Vikhrenko [5,6] can be of extreme interest in understanding the Mg-ion insertion kinetics into Mo_6S_8 Chevrel phase electrodes and, hence, in understanding major differences between intercalation of single and divalent cations into transition metal oxides and sulfides hosts.

2. Experimental

The experimental details related to EIS characterization of Li and Mg ions insertion into the Chevrel phase electrodes has been already reported [3]. The electrolyte solutions for Mg insertion studies comprised of Mg salts of the general formula $Mg(AlCl_{(4-n)}R_n)_2$ (with R = alkyl group) possessing a relatively high anodic stability, dissolved in THF. Their preparation and properties were already reported [1,7]. $Mg(AlCl_2{-}EtBu)_2$, abbreviated here as DCC, was used as the electrolyte. Usually we used 0.25 M $Mg(AlCl_2BuEt)_2$/THF solutions (DCC/THF). The electrolyte solution for Li ions insertion was 1 M $LiClO_4$ in propylene carbonate (PC). The cathodes comprised the following components: 6–15 mg Mo_6S_8, 10% carbon black and 10% PVdF (by weight), coated onto 1 cm × 1 cm stainless steel foils. Strips of Li or Mg foil served as counter and reference electrodes. The cells were operated under highly pure argon atmosphere in M. Braun Inc. glove boxes and were thermostated at different temperatures, with an accuracy of ±0.5 °C.

For detailed electrochemical impedance characterizations of Mg and Li-ion insertion into Mo_6S_8 we used a computerized potentiostat–galvanostat Eco Chemie Model 20 Autolab, supplied with a FRA module. The collection of data was controlled by the GPES Version 4.8 Eco Chemie B.V. Software (Utrecht, The Netherlands). The electrodes impedance was measured between 60 kHz down to 5 mHz (in this order) after a complete equilibration of the electrodes at a variety of predefined potentials. High-resolution spectra were measured around a large number of equilibrium potentials in order to identify processes and states of interest. The impedance spectra collected for both ions insertions, related only to well-cycled electrodes, in order to exclude possible irreversible processes or processes with temporary slow dynamics.

3. Results and discussion

Fig. 2 shows typical Nyquist plots related to Li insertion into $Li_xMo_6S_8$ ($0 < x < 0$) Chevrel phase electrodes. The

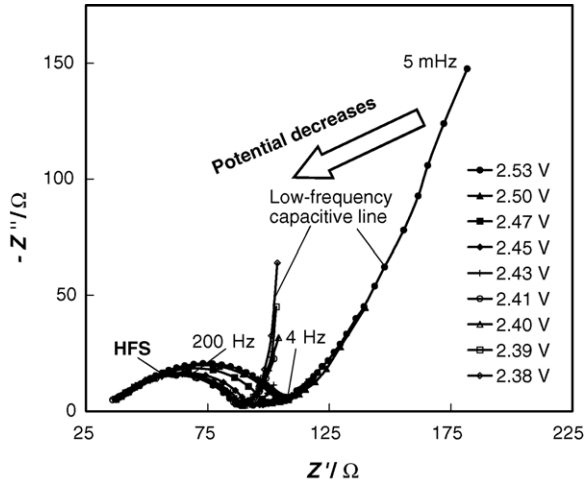

Fig. 2. Nyquist plots for Li ions insertion into a Mo_6S_8 electrode, for the entire range of intercalation potentials (the direction of decreasing the potential is indicated by the arrow).

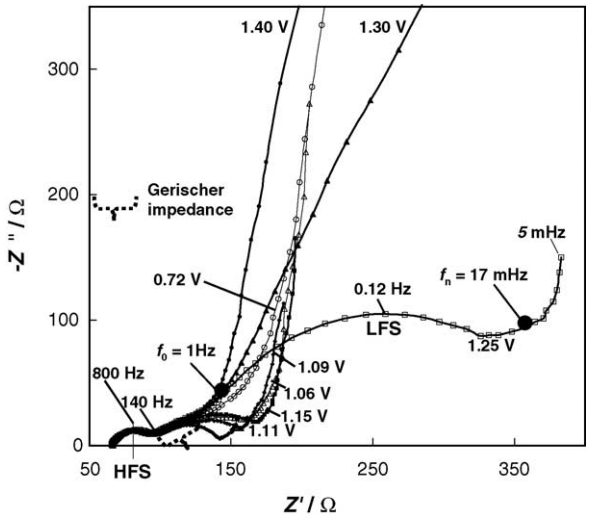

Fig. 3. Impedance spectra measured from a Mo_6S_8 Chevrel electrode for Mg ions insertion at different potentials as indicated. Solid black circles mark two different experimental characteristic frequencies, f_o and f_n, in the high and in the low-frequency domain, respectively. The most prominent features of the impedance spectra are the LFS and the Gerischer impedance in the low and the high-frequency domain, respectively; the high-frequency semicircle was discussed in detail in an earlier paper [3].

spectra comprise high-frequency semicircle (HFS) which relates to charge transfer (no surface films or other complicated surface phenomena in this case), and a low-frequency Warburg-type element which reflects the solid-state diffusion and, finally, at the very low frequencies, the $-Z''$ versus Z' plots become steep and reflect the differential intercalation capacitance ($C_{dif} = -1/\omega Z'', \omega \to 0$). These spectra reflect the smooth intercalation of Li ions into this host, which occurs with no complications as charge-trapping, slow diffusion or pronounced surface resistance (as is the case for Li insertion into transition metal oxide hosts such as Li_xNiO_2, Li_xCoO_2, $Li_xMn_2O_4$ spinel, etc.).

At the beginning of Mg-ions intercalation (see the relevant Nyquist plots for Chevrel phase electrode at the potentials 1.4 and 1.3 V in Fig. 3) the diameter of the LFS is so large that practically only an arc can be obtained down to the lowest measuring frequency of 5 mHz (for details see ref. [3]). While the initial Mg intercalation involves the full capacity of the host (2 Mg ions per Mo_6S_8 unit), the reversible intercalation level of Mo_6S_8 with Mg-ions at RT (25 °C) is around $x = 1.6$–1.7 [1], i.e. by 15–20% less than the theoretical value $x = 2$. At the potential of 1.25 V the host accommodates the amount of Mg-ions corresponding to $x = 0.6$–0.7 [1] so that starting from this potential only, a well-developed LFS is formed, which transforms into a purely capacitive vertical line in the limit of the lower frequencies (see Fig. 3). A very interesting feature is observed as the frequency increases: the LFS rather abruptly transforms to a line described approximately by a semi-infinite Warburg behavior (see Fig. 3 and ref. [3] for details). Thus, two characteristic frequencies (shown on the curve in Fig. 3 by the solid circles), one related to the above border between the LFS and the Warburg domain, and the other (at lower frequencies) located between the LFS and the limiting capacitive line can be experimentally distinguished.

Further decrease in potential (i.e. an increase in the intercalation level) results in a continuous decrease of the diameter of the LFS, the higher frequency domain becomes more and more similar to the Gerischer-type impedance (see Fig. 3 and ref. [3]), which is marked in Fig. 3 by dotted curly brace. The Gerischer domain is located between the high-frequency semicircle and the LFS. The former HFS relates to the interfacial charge transfer, not in a simple way, because of the complicated character of the chemical equilibria in the DCC/THF solution and possible adsorption processes [3]. It will be further ignored because herein we focus on the solid-state diffusion with entrapment of ions in the host [8]. It is of great interest that as the potential approaches the value of 0.72 V, which is close to the limit of Mg-ions insertion into the Chevrel phase electrode at ambient temperature ($x = 1.6$–1.7), the high-frequency limit of the relevant impedance does not include the semicircles anymore (neither the LFS nor the curved Gerischer-type impedance): the impedance behavior is rather similar to a semi-infinite Warburg line transforming to a vertical capacitive line at lower frequencies (Fig. 3).

All the above-described features of the impedance behavior during Mg-ions insertion into Mo_6S_8 Chevrel phase electrodes can be nicely semi-quantitatively explained on the basis of the two-state model of Bisquert and Vikhrenko [5], modified as discussed below. Originally, this model suggests that hosts suitable for intercalation processes may contain two types of sites, the deep (or hollow) and shallow ones. At the beginning of intercalation, the hollow sites with the limited ion mobility (because of the higher diffusion barrier) are occupied. With a further increase in the intercalation level, the shallow sites (with much lower diffusion barrier) start to be populated. It should be emphasized that adoption of such models for describing the intercalation of Mg ions into Mo_6S_8 is in line with precise crystallographic data about these materials. This clearly shows that there are two types of sites for bivalent ions insertion in Chevrel phases, which are different from each other in their energetics (two sets of six-sites rings, see Section 1). The overall complex plane impedance of the intercalation system containing two types of sites ($Z(s)$) can be conveniently presented as a function of the angular frequency (ω) in the form (see ref. [5]):

$$Z(s) = R_o \left(\frac{\omega_n^*(s)}{s} \right)^{1/2} \coth \left[\left(\frac{s}{\omega_n^*(s)} \right)^{1/2} \right], \quad (1)$$

where $s = j\omega$, and the diffusion resistance R_o (related to the motion of the intercalated ions between the shallow sites) relates to the corresponding diffusion coefficient, D_o, through the intercalation capacitance of the shallow sites, C_o, and the characteristic frequency, ω_o:

$$\omega_o = \frac{D_o}{L^2} = \frac{1}{R_o C_o}. \quad (2)$$

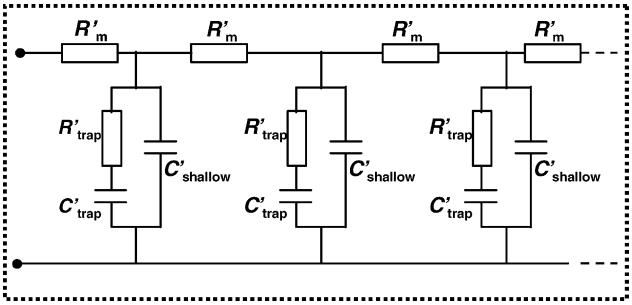

Fig. 4. Transmission line representation of coupling between the diffusion and ions trapping in the host material of an intercalation electrode.

Here L is the electrode thickness. According to the two-state model [5], the intercalated ions move by ordinary diffusion mechanism between the shallow sites, interacting, at the same time, with the hollow sites and becoming immobilized for a lapse of time. The characteristic frequency related to ion trapping and release at the hollow sites, ω_t, defines an effective, frequency dependent diffusion coefficient, $D_n^*(s)$, through the ratio of the intercalation capacitances describing the occupation of the hollow and the shallow sites, C_{trap} and C_o, respectively:

$$D_n^*(s) = \frac{\omega_o L^2}{1 + [1 + (s/\omega_t)]^{-1}(C_{trap}/C_o)} \quad (3)$$

Note also that the diffusion motion coupled with ions trapping on the hollow sites can be presented by a characteristic frequency as follows:

$$\omega_n^*(s) = \frac{D_n^*(s)}{L^2} \quad (4)$$

with $D_n^*(s)$ obtained from Eq. (3). Thus, defined $\omega_n^*(s)$ should be inserted in Eq. (1) for the final calculation of the electrode impedance for the case of the coupled diffusion with ion trapping.

The impedance obtained with the use of Eq. (1) can be better understood in terms of the transmission line representation (see Fig. 4) with the two transverse branches in parallel comprising the intercalation capacitance of the shallow sites, C_o, and the intercalation capacitance of the hollow sites, C_{trap}, in series with the relevant kinetic parameter, namely, the trapping resistance, R_{trap}. An obvious equation expresses the additive (cumulative) character of the total capacitance observed at very low frequencies: $C_{tot} = C_o + C_{trap}$.

Modeling impedance spectra of an intercalation electrode with two different energy sites through Eqs. (1)–(4) requires four independent parameters: ω_o, ω_t, C_{trap}, and C_o. The main problem of the modeling is a reasonable guess of how these parameters may depend on the electrode potential (or intercalation level). It is the general property of the family of two states models (e.g. proposed by Bisquert and Vikhrenko [5], and by Chvoj et al. [9,10]) that the chemical diffusion coefficient of the inserted ions experiences a sharp increase in the vicinity of a certain intercalation level separating the end of occupation of the hollow sites with the ions and the beginning of occupation of the shallow sites (the characteristic frequency also increases). We assume that the impedance spectrum measured at 1.25 V (see Fig. 3) approximately fulfills this condition. In order to reproduce the impedance spectra in the vicinity of this transition, we assumed that the only parameter, which changes with potential is the characteristic frequency of the trapping process, ω_t (this is the main modification of the original theory of Bisquert and Vikhrenko [5]). We believe that this assumption is specific of the Mg-ions intercalation into the Chevrel phase (in which ion-trapping is very pronounced) since Mg-ions are divalent, and as a result, an increase in the intercalation level beyond the above discussed boundary between the hollow and shallow sites must substantially increase the probability (velocity) of the ion-hopping from the hollow (inner six-sites ring) to the shallow position (outer six-sites ring) because of the drastically increasing electrostatic repulsion between the Mg-ions. Notice that the intercalation of single charged Li-ions into the same Chevrel phase electrode did not reveal a trace of ionic trapping (see Fig. 2) [3]. For the purpose of a qualitative comparison of the model calculations with the experimental curves, we assumed an augmentation in the ω_t by more than 3 orders of magnitude as the intercalation level increases (see captions to Fig. 3).

Fig. 5 ("a" refers to the whole frequency domain whereas "b" enlarges, for clarity, the high-frequency domain) shows theoretical impedance spectra calculated with the use of Eqs. (1)–(4) as a function of the parameter ω_t (or, equivalently, as a function of the charge-trapping resistance, R_{trap}, obtained from the equation: $R_{trap} = 1/(\omega_t C_{trap})$ [3] and indicated in the figure). In the curve related to $R_{trap} = 500\ \Omega\ cm^2$ three characteristic frequencies, namely, ω_o, ω_t, and ω_n (the latter was found as the boundary frequency separating the LFS and the low-frequency, capacitive line on the related impedance spectrum as indicated). It is seen that this case corresponds to very slow trapping kinetics of the initial Mg-ions insertion ($\omega_t \ll \omega_o$), thus the high-frequency impedance shows a pattern of the classical semi-infinite Warburg behavior (see Fig. 5b and the location of ω_o for $R_{trap} = 500\ \Omega\ cm^2$) since at these high frequencies the diffusion of ions via the shallow sites is unperturbed by the slower trapping kinetics [3]. At lower frequencies, the Mg-ions trapping appear as the LFS, formed by a parallel combination of C_o and R_{trap} (see the equivalent circuit in Fig. 4).

The decrease in the values of the parameter R_{trap} (i.e. the increase in ω_t) obviously results in a considerable decrease in the diameter of the LFS (see Fig. 5a and b). As a result, the impedance spectra acquire a new feature of Gerischer-type in the high-frequency domain followed by a kind of the semi-infinite Warburg behavior, and finally, vertical capacitive line as the frequency decreases. These features, first established by Bisquert [8], can be easily understood from the transmission line properties shown in Fig. 4 and from the values of the characteristic frequencies ω_t and ω_o: as the operative frequency is high as well as C_{trap}, the reactance due to C_{trap} is

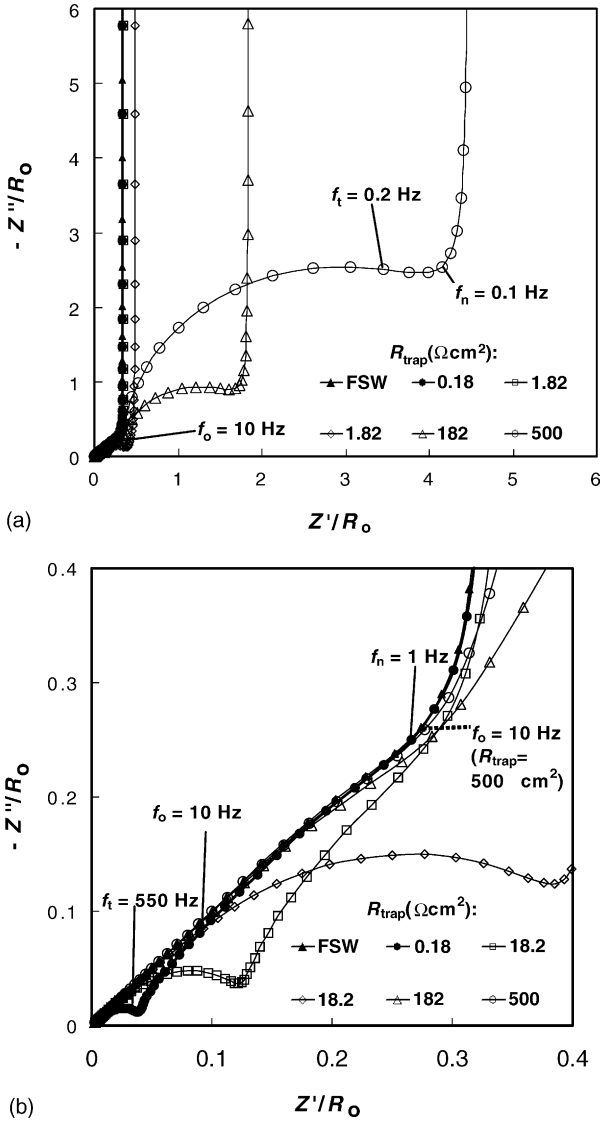

Fig. 5. Theoretical impedance spectra calculated with the use of Eqs. (1)–(4) showing the whole frequency domain from 320 kHz to 0.1 mHz (a) and enlargement of the high-frequency domain (b). The following parameters were used: $R_o = 100\ \Omega\,cm^2$, R_{trap} (as indicated), C_o and $C_{trap} = 0.001$ and $0.01\ mF\,cm^{-2}$, $f_o = 10$ Hz. f_{trap} and f_n are also indicated.

small compared to R_{trap}. In this case, the latter quantity is much less than R_o, hence $\omega_t \gg \omega_o$ (see the values indicated in Fig. 5b), and the concentration profile of the intercalated ions decay before the species reach the boundary at the current collector (the Gerischer impedance) [8]. This impedance spectrum has two semi-infinite Warburg regions having different prefactors related to ω_o and ω_n at high and medium frequencies, respectively [5]. When R_{trap} decreases virtually to zero (i.e. the traps disappear), the impedance response will be reflected by the classical finite-space Warburg element (FSW) with one single characteristic frequency ω_o (see Fig. 5b). Comparison between the model curves in Fig. 5a and b and the experimental ones obtained for the Mg-ions insertion into the Chevrel electrode (Fig. 3, compare also the limiting case: FSW versus plot measured at 0.72 V) reveal their qualitative similarity.

4. Conclusion

The Chevrel phase $M_xMo_6S_8$ ($0 < x < 4$ for monovalent ions and $0 < x < 2$ for divalent ions) is a very good probe for the study of general phenomena related to electrochemical intercalation processes. This host has several types of sites differing from each other by their energetics and, hence, by barriers for diffusion of the intercalants. In the case of Li insertion, the difference in sites is reflected only by the reversible redox-potentials while the kinetics of Li insertion is fast in all its stages. In contrast, Mg ions insertion is more complicated and involves charge-trapping at the beginning of intercalation and at the end of deintercalation. Impedance spectra related to Mg-ions insertion into the Mo_6S_8 Chevrel phase electrode have very peculiar behavior with a Gerischer-type impedance at high frequencies and low-frequency semicircle, the latter being especially pronounced at the beginning of intercalation. Two experimental diffusion time constants, one related to the high-frequency (ω_o), the other to the low-frequency domain (ω_n) can be easily identified on the experimental impedance spectra. A recent model for two non-equivalent lattice sites with two different energy barriers (Bisquert and Vikhrenko [5]) has been applied to reproduce semi-quantitatively the above impedance features. The most essential in our analysis of the trapping effect of Mg-ions in the Chevrel phase electrode is the assumption that the increase in the intercalation level (i.e. the decrease in potential) can be reproduced by a decrease in the trapping resistance, R_{trap} (i.e. by the increase in ω_t). This assumption seems to be in good agreement with the divalent nature of Mg-ions, which decrease the diffusion barrier of the trapped ions due to a much higher electrostatic repulsion (the inner six-sites ring) by pushing them into the shallow sites (the outer six-sites ring), as intercalation progresses. This explains well the fact that the first stage of Mg intercalation is relatively slow, while the second stage is fast.

Acknowledgment

A partial support for this study was obtained by the ISF (Israel Science Foundation).

References

[1] M.D. Levi, E. Lancry, H. Gizbar, Z. Lu, E. Levi, Y. Gofer, D. Aurbach, J. Electrochem. Soc. 151 (2004) A1044.
[2] M.D. Levi, E. Lancry, H. Gizbar, Y. Gofer, E. Levi, D. Aurbach, Electrochim. Acta 49 (2004) 3201.
[3] M.D. Levi, H. Gizbar, E. Lancry, Y. Gofer, E. Levi, D. Aurbach, J. Electroanal. Chem. 569 (2004) 211.

[4] C. Ritter, E. Gocke, C. Fischer, R. Schollhorn, Mater. Sci. Res. Bull. 27 (1992) 1217.
[5] J. Bisquert, V.S. Vikhrenko, Electrochim. Acta 47 (2002) 3977.
[6] J. Bisquert, Electrochim. Acta 47 (2002) 2435.
[7] H. Gizbar, Y. Vestfrid, O. Chusid, Y. Gofer, H.E. Gottlieb, V. Marks, D. Aurbach, Organometallics 23 (2004) 3826.
[8] J. Bisquert, J. Phys. Chem. B 106 (2002) 325.
[9] Z. Chvoj, H. Conrad, V. Chab, Surf. Sci. 376 (1997) 205.
[10] Z. Chvoj, H. Conrad, V. Chab, Surf. Sci. 442 (1997) 455.